Geocatalytic uptake of ozone onto natural mineral dust

Xianjie Wang, Manolis Romanias, Frederic Thevenet, Antoine Rousseau

▶ **To cite this version:**

Xianjie Wang, Manolis Romanias, Frederic Thevenet, Antoine Rousseau. Geocatalytic uptake of ozone onto natural mineral dust. Catalysts, 2018, 8 (7), pp.263. 10.3390/catal8070263 . hal-02406809

HAL Id: hal-02406809
https://hal.science/hal-02406809v1

Submitted on 23 Feb 2024

HAL is a multi-disciplinary open access archive for the deposit and dissemination of scientific research documents, whether they are published or not. The documents may come from teaching and research institutions in France or abroad, or from public or private research centers.

L'archive ouverte pluridisciplinaire **HAL**, est destinée au dépôt et à la diffusion de documents scientifiques de niveau recherche, publiés ou non, émanant des établissements d'enseignement et de recherche français ou étrangers, des laboratoires publics ou privés.

catalysts

MDPI

Communication

Geocatalytic Uptake of Ozone onto Natural Mineral Dust

Xianjie Wang [1], Manolis N. Romanias [2], Frédéric Thévenet [2,*] and Antoine Rousseau [1,*]

[1] LPP, CNRS, Ecole Polytechnique, Sorbonne Université, Université Paris-Sud, Observatoire de Paris, Université Pairs-Saclay, F-91128 Palaiseau, France; xianjie.wang@lpp.polytechnique.fr

[2] IMT Lille Douai, SAGE, Université de Lille, F-59500 Douai, France; emmanouil.romanias@imt-lille-douai.fr

* Correspondence: frederic.thevenet@imt-lille-douai.fr (F.T.); antoine.rousseau@lpp.polytechnique.fr (A.R.); Tel.: +33-(0)-1-69-33-59-63 (A.R.)

Received: 4 June 2018; Accepted: 26 June 2018; Published: 29 June 2018

Abstract: Beyond tailored and synthetic catalysts sought out for ozone decomposition, mineral dusts provide naturally mixed metal oxide materials. The steady-state uptake of O_3 evidenced across a wide concentration range signifies the catalytic decomposition of O_3. The geocatalytic properties of such natural mineral dust open up new perspectives in atmospheric chemistry and catalytic processes.

Keywords: mineral dust; metal oxide; ozone; catalytic uptake; geocatalysis

1. Introduction

Ozone is a key reactive species for both fundamental and applied research fields, such as atmospheric environments, ecosystems [1,2], medicine [3,4], plasma catalysis [5,6], and industry. Due to environmental concerns and the widespread applications of ozone-based remediation techniques, over the last two decades, the interactions of ozone with metal oxides, such as Al_2O_3 [7–11], MnO_2 [12,13], Fe_2O_3 [7,14], SiO_2 [15,16], CaO [17], TiO_2 [18], and MgO [19], have been extensively studied. Most of the investigated synthetic oxides exhibit decomposition properties towards ozone. With the aim of optimizing ozone catalytic decomposition, novel catalysts based on tailored metal oxide combinations with controlled morphologies have been synthesized using complex methods and processes [20,21]. Noticeably, the production expenses (e.g., materials and solvent costs, energy use, waste management, and disposal) and sales of catalysts is estimated to be US$11 billion per year, and about 80% of the chemical processes in industry involve catalysts [22].

Recent studies related to heterogeneous atmospheric chemistry focused on the ozone interaction with suspended and transported crustal dust in the atmosphere have highlighted these natural mineral materials. Natural mineral dusts constitute 50% of the annual aerosol emissions on Earth, corresponding to two billion tons of suspended inorganic particulate materials [23]. These massive emissions are mostly related to sandstorms in desert areas and volcanic eruptions. Interestingly, natural mineral dust participates directly in atmospheric activities and significantly interacts with ozone [11,24–26]. In spite of the fact that geochemists introduced the concept of geocatalysis in the 1990s, referring to possible catalytic properties of Earth crustal materials, such catalytic potential has not been experimentally evidenced so far [27]. Since mineral dust chiefly consists of a mixture of metal oxides, including an abundance of SiO_2, $CaCO_3$, Al_2O_3, Fe_2O_3, and TiO_2 among others [28,29], natural dust is a material of interest regarding the catalytic decomposition of ozone. In the field of heterogeneous atmospheric chemistry, ozone uptake onto natural mineral dust is generally reported and described as a transient phenomenon, and is partially characterized by atmospheric chemists but not limited to, atmospheric conditions (thus evidencing catalytic properties of the geomaterial

regarding ozone decomposition). The utilization of natural mineral dust can not only achieve great economic benefits, but also provide new insights about environmental issues.

The objectives of the current study are: (i) to investigate whether natural mineral dust exhibits catalytic properties towards ozone, and if so, (ii) to evaluate whether the catalytic performance of natural dust could be comparable with conventional materials used as catalysts. Within that framework, carefully designed kinetic experiments were carried out to investigate the uptake efficiency of natural mineral dust collected from the Gobi Desert towards ozone at room temperature and under atmospheric pressure using a fixed bed reactor. The Gobi dust was used as a natural material probe, aiming to evaluate its decomposition efficiency towards ozone (without excluding that other natural dusts could have similar or even higher decomposition efficiencies).

2. Results and Discussion

A typical profile of ozone uptake onto the selected Gobi mineral dust is reported in Figure 1a. Prior to the experiment, the sample was thermally pretreated at 150 °C under zero air for 30 min to remove pre-absorbed species from the sample surface, but not to induce any phase or morphology change. The sample was then cooled down to room temperature under zero air flow. When the pretreatment was over, the reactor with the dust sample inside was isolated and the ozone flow was driven through the bypass line to be measured directly by the ozone analyzer. After equilibration, a constant ozone concentration (i.e., initial ozone concentration: $[O_3]_0$) was reached at the bypass outlet. The ozone flow is then directed into the U-shape reactor, i.e., in contact with the investigated sample. An immediate decrease of O_3 concentration monitored at the reactor outlet was observed, denoting its initial uptake onto the Gobi dust surface. Preliminary blank experiments showed that ozone reaction with the quartz substrate was negligible and does not impact measurements. Beyond the abrupt O_3 concentration drop at the initial stage of interaction with dust, a progressive increase of O_3 concentration was observed as the interaction with Gobi dust proceeded. As reported in Figure 1a, a steady-state concentration of ozone was reached at the reactor outlet within 2 h. Interestingly, if ozone flow remains in contact with the dust bed, O_3 concentration remained noticeably lower than $[O_3]_0$, corresponding to a constant consumption of ozone onto the natural mineral dust sample. Beyond the results reported in Figure 1a, the constant consumption of ozone (i.e., the steady-state uptake of ozone) has been evidenced for more than 15 h, without any noticeable deviation. Thereafter, the ozone flow was re-directed to the bypass line to validate the stability of generated $[O_3]_0$.

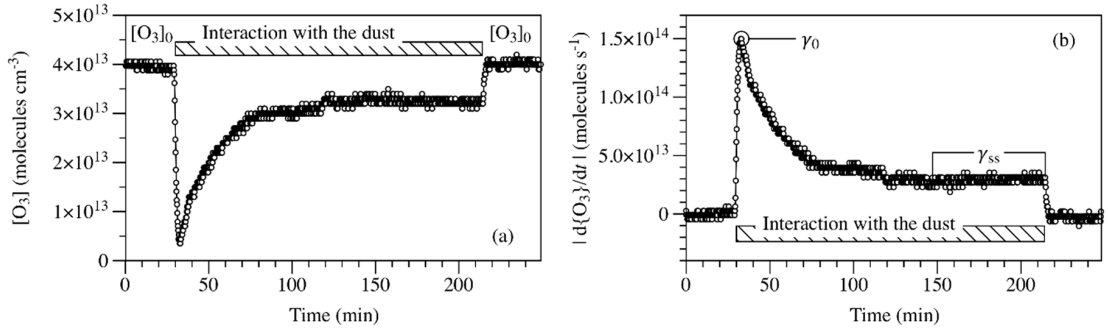

Figure 1. (**a**) Typical profile of the uptake of 4×10^{13} molecule cm^{-3} O_3 (i.e., 1.6 ppm) displayed by ozone concentration variation as a function of time, on 100 mg Gobi dust sample at room temperature and atmospheric pressure using the fixed bed reactor; $[O_3]_0$ is the initial inlet ozone concentration measured as ozone was directed through the bypass line without interacting with the dust samples. (**b**) Corresponding absolute ozone molecule flow taken up by the 100 mg Gobi dust sample, expressed in molecule s^{-1}; the datasets used to calculate γ_0 and γ_{ss} are indicated.

According to the concentration profile reported in Figure 1a, Gobi dust clearly exhibits two distinct uptake modes overall: (i) the transient initial uptake and (ii) the continuous steady-state uptake of

ozone that evidences the catalytic properties of the selected dust and supports the initial concept of geocatalysis. Based on the measurements reported in Figure 1a, the calculation of the absolute ozone uptake $|d\{O_3\}/dt|$ expressed in molecule s^{-1} is reported in Figure 1b, where $\{O_3\}$ denotes the number of ozone molecules. $|d\{O_3\}/dt| = -\Gamma([O_3] - [O_3]_0)$, where Γ represents the gas flow in $cm^3\ s^{-1}$ and $[O_3]$ and $[O_3]_0$ are the ozone concentration at time t and the initial ozone concentration, expressed in molecules cm^{-3}.

According to the atmospheric heterogeneous interaction studies, the absolute number of ozone molecules lost per second from gas phase due to the interaction of the ozone molecules with the mineral surface depends on the effective surface of the dust, the average molecular speed of ozone molecules, and the uptake coefficient [30–33]; this can be determined from Equation (1):

$$\left|\frac{d\{O_3\}}{dt}\right| = \frac{1}{4}\gamma c A_{BET}[O_3]_0 \quad (1)$$

where A_{BET} is the total and effective surface area (cm^2), referring to the BET surface, provided by the dust sample inserted in the U-shape reactor; γ is the uptake coefficient which expresses gas-to-surface transfer probability; c is the mean molecular speed of O_3 molecules, $c = 100 \times \sqrt{8kT/\pi M}$ ($cm\ s^{-1}$) with k the Boltzmann constant ($J\ K^{-1}$), T the operating temperature (K) and M the molecular mass of O_3 (kg). Under our experimental conditions, $c = 3.6 \times 10^5$ $cm\ s^{-1}$. The approximation used in Equation (1) assumes the uptake probability $\gamma \ll 1$, which is the case in the present paper. The uptake probability (γ) can be derived from Figure 1b and Equation (2) [30,31]:

$$\gamma = \frac{4(d\{O_3\}/dt)}{cA_{BET}[O_3]_0} \quad (2)$$

The estimation of the uptake coefficient is a macroscopic probability, which does not require any assumption regarding the surface reaction order or reaction mechanisms. For the two different uptake states, initial uptake coefficients (γ_0) are determined using the data collected during the very first seconds of dust sample exposure to O_3, while the steady-state uptake coefficients (γ_{ss}) are determined along the steady-state uptake regime. The data sets used for the calculations of γ_0 and γ_{ss} are indicated in Figure 1b. It has been validated previously that γ_0 and γ_{ss} are independent of the mass of the dust in our experiments.

The determined γ_0 and γ_{ss} of ozone on Gobi dust have been plotted as a function of initial ozone concentration $[O_3]_0$, and varied from 20 ppb to 10 ppm in Figure 2. Both γ_0 and γ_{ss} decrease with $[O_3]_0$, meaning that the fraction of the ozone molecular flow taken up by the surface of the natural sample decreases as ozone concentration increases.

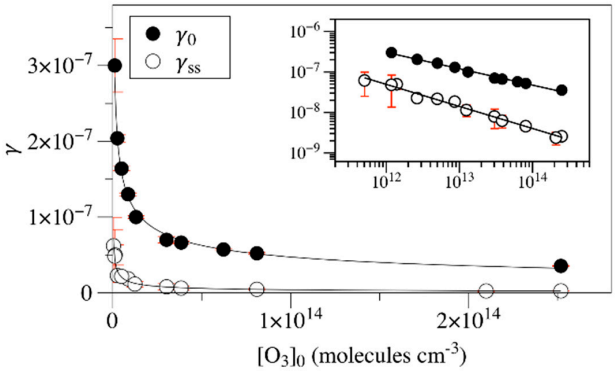

Figure 2. γ_0 and γ_{ss} of ozone on Gobi dust as a function of $[O_3]_0$. The solid lines are power function fittings of γ and $[O_3]_0$. The embedded figure corresponds to the logarithmic display mode. Experiments were carried out at room temperature and atmospheric pressure using a fixed bed reactor. Error bars were determined from the overall experimental dispersion.

The dependence of uptake coefficients on ozone initial concentration can be described by an analytical fit of power functions reported by solid lines in Figure 2 and is given by Equation (3) and Equation (4). where $[O_3]_0$ is in molecules cm^{-3}:

$$\gamma_0 = 0.022[O_3]_0^{-0.4} \quad (3)$$

$$\gamma_{ss} = 0.171[O_3]_0^{-0.5} \quad (4)$$

Similar dependence patterns for γ_0 and γ_{ss} on $[O_3]_0$ have been reported for other materials, such as Al_2O_3 [11,34]. Since uptake coefficients depict the probability for a molecule to be taken up by a surface when striking it, the decreasing trends in Figure 2 suggest a finite ability of the sample surface to decompose ozone in terms of molecules processed per time and surface unit. To that regard, the catalytic character of ozone uptake by Gobi dust during the steady-state uptake regime can be further characterized by the uptake rate r_{ss} (molecules cm^{-2} s^{-1}) as defined by Equation (5).

$$r_{ss} = \frac{\gamma_{ss} c [O_3]_0}{4} \quad (5)$$

Compared to γ_{ss}, r_{ss} reflects the kinetic of ozone decomposition onto the natural mineral sample. The specific dependence of r_{ss} on ozone initial concentration $[O_3]_0$ is reported in Figure 3. The profile can be modeled using a power function, as reported in Equation (6), revealing a fractional reaction order of 0.5 regarding the catalytic decomposition process of ozone onto Gobi dust.

$$r_{ss} = 363 \times [O_3]_0^{0.5} \quad (6)$$

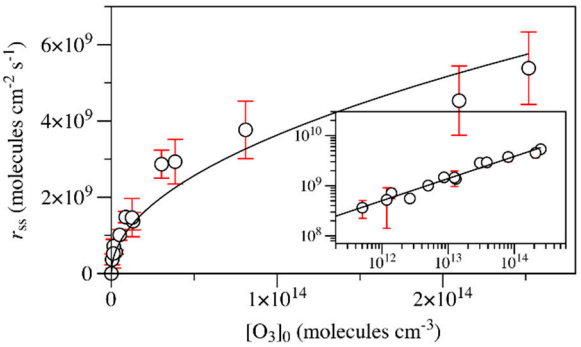

Figure 3. Evolution of r_{ss} as a function of ozone initial concentration $[O_3]_0$. The solid line displays the power function fitting of r_{ss} and $[O_3]_0$. The embedded figure corresponds to the logarithmic display mode. Experiments were carried out at room temperature and atmospheric pressure using a fixed bed reactor. Error bars were determined from the overall experimental dispersion.

Figure 3 evidences that ozone steady-state uptake onto a Gobi dust sample is characterized by mixed orders depending on the considered ozone concentration range. Considering the whole investigated concentration range, Equation (6) provides the global order with a value of 0.5. However, a first order kinetic can be observed for ozone concentrations lower than 10^{13} molecule cm^{-3}. At higher concentrations, a lower reaction order characterizes the surface process. A maximum reaction rate is not fully reached within the investigated concentration range, and reaction rate uncertainties would not allow a reliable extrapolation to obtain the zero-order reaction rate value on the highest investigated concentrations.

The uptake of ozone onto mineral dust, as well as other metal oxides, has been previously investigated by other authors. Most of the investigations were conducted with a Knudsen cell under a total pressure generally lower than 10^{-6} bar, and dry conditions with an ozone concentration of a few

ppb. These conditions are relevant to neither the real atmosphere, nor common air treatment processes. In the latest evaluation of the International Union of Pure and Applied Chemistry (IUPAC) [31], it has been clearly mentioned that uptake coefficients strongly depend on the following experimental conditions: (i) the gas phase concentration of the molecule (uptake decreases as the concentration of the gas increases), (ii) the total pressure used to carry out the experiment, (iii) the exposure time used to determine the uptake coefficient (i.e., at the initial stage or after achieving equilibrium conditions), (iv) the temporal resolution of the instrument used to monitor the gas concentration of the reactor outlet, and (v) the residence time of the molecule in the reactor. Therefore, comparisons of uptake coefficients should be made between studies under the same or close conditions.

Alebić-Juretić et al. have investigated the decomposition of 100 ppb ozone on powders of pure metal oxides, as well as another mineral dust from the Sahara Desert using a fluidized bed reactor under atmospheric pressure and at room temperature [15]. Interestingly, the investigated single oxide materials are also present in the Gobi dust composition. Based on the data reported by the authors, γ_{ss} and r_{ss} of O_3 can be calculated. Processed results were compared with Gobi dust for the same ozone concentration and reported in Table 1.

Table 1. Comparison of γ_{ss} and r_{ss} determined in the presence of 100 ppb of ozone on natural Gobi dust, SiO_2, Al_2O_3 and $CaCO_3$ under atmospheric pressure and at room temperature.

Materials	γ_{ss}	r_{ss} (Molecules cm^{-2} s^{-1})	Ref.
SiO_2	3.74×10^{-10}	7.82×10^{6}	[15]
Al_2O_3	3.79×10^{-9}	8.53×10^{7}	[15]
$CaCO_3$	$<<10^{-10}$	$<<2.40 \times 10^{6}$	[15]
Saharan dust	0	0	[15]
Gobi dust	2.28×10^{-8}	5.60×10^{8}	This work

As listed in Table 1, both γ_{ss} and r_{ss} evidence that Gobi dust, as a geocatalyst, exhibits higher catalytic properties towards ozone decomposition than the individual metal oxides contained in Gobi dust (SiO_2, Al_2O_3 and $CaCO_3$). The geocatalytic decomposition rate of ozone onto natural mineral dust exceeds the decomposition rates determined for Al_2O_3 and SiO_2 by one and two orders of magnitude, respectively. As for Saharan dust, the authors have found the ozone concentration returning to the initial value after 50 min of exposure with the fluidized bed reactor, which is contrary to our result where Gobi dust shows continued steady uptake of ozone.

Furthermore, in Table 2, Gobi dust is compared with MnO_2 (which is known as one of the most effective metal oxide for ozone decomposition). The data for MnO_2 are based on the experiments conducted by Jia et al. [13] on 14 ppm of ozone onto MnO_2 under atmospheric pressure and at room temperature with a flow-through tube reactor. Interestingly, the most widespread ozone decomposition catalyst (MnO_2) showed a higher but comparable γ_{ss} value.

Table 2. Comparison of γ_{ss} and r_{ss} determined in the presence of 10 ppm of ozone on natural Gobi dust and 14 ppm of ozone on MnO_2 under atmospheric pressure and at room temperature.

Materials	γ_{ss}	r_{ss} (Molecules cm^{-2} s^{-1})	Ref.
α-MnO_2	$>2.5 \times 10^{-8}$	$>7.9 \times 10^{10}$	[13]
β-MnO_2	8.1×10^{-8}	2.6×10^{11}	[13]
γ-MnO_2	2.6×10^{-8}	8.2×10^{10}	[13]
Gobi dust	2.6×10^{-9}	5.8×10^{9}	This work

3. Experimental Section

The dust sample was collected from the Gobi Desert, Ningxia Province, in China. The Gobi Desert is the second most important source of atmospheric mineral dust on Earth, after the Sahara

Desert [35]. The collected sample corresponds to a natural aeolian deposit; it has only been sieved in order to select the fraction below 100 µm. Such a granulometric fraction provides a specific surface area comparable with the typical specific surface areas observed with commercially available and synthetic metal oxides usually used in catalytic and sorptive processes. The BET surface of the sample, measured by a sorption analyzer using nitrogen as adsorbate gas, is 10.5 ± 2.0 m^2 g^{-1}. The relative abundances of mineral oxide phases in Gobi dust determined by XRD spectroscopy combined with ICP mass spectrometry are 55.0% SiO_2, 17.8% $CaCO_3$, 10.5% $NaAlSi_3O_8$, 6.9% Al_2O_3, 2.6% Fe_3O_4, 1% TiO_2 and 6.2% of uncounted fraction [36].

To determine the uptake efficiency of the selected dust regarding ozone, the experimental setup used consisted of three main parts: (i) an ozone flow generation system combining a dielectric barrier discharge (DBD) reactor to provide ppm levels of ozone and a UV light ozone generator for ppb-level ozone production, (ii) a U-shape fixed bed reactor, and (iii) an ozone analyzer (Figure 4). This experimental set up has been used extensively in the past to investigate the heterogeneous interaction/reaction of volatile organic compounds (VOCs) and inorganic species with natural mineral dusts and proxies [36–40], and thus only a brief description is provided.

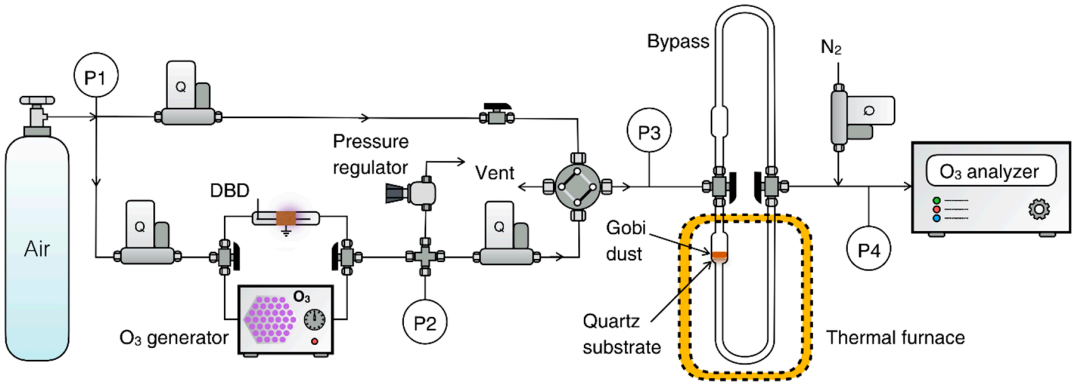

Figure 4. General scheme of the experimental setup.

Zero dry air from cylinders provided and certified by *Air Liquide* were used as the main carrier gas. Ozone was generated by flowing air through the DBD reactor or the UV-light ozone generator. A pressure regulator was used to provide enough upstream pressure while keeping the pressure inside the gas flow generation system stable, which is necessary for stable ozone production. The four-way valve allowed fast switching between ozone flow and zero air flow. The dust sample was placed on a 0.82 cm^2 quartz sample holder inside the U-shape fixed bed reactor, which has a volume of 12 mL. The U-shape reactor can be moved to a furnace to perform thermal treatments of the reactor and/or investigated sample. A bypass line of the same volume was connected to the U-shape reactor in parallel. The reactor downstream was coupled with the ozone analyzer (*Environnement* S.A O342e) to measure the gas phase ozone concentration at the outlet of the reactor or bypass line. The instrument is characterized by an accuracy of 0.1 ppb and a detection limit of 0.2 ppb. Experiments were conducted at room temperature and atmospheric pressure using a continuous gas flow rate of 250 sccm through the U-shape reactor. An extra nitrogen flow of 750 sccm was merged upstream of the ozone analyzer to meet its optimal work flow rate, which is around 1000 sccm.

4. Conclusions

In conclusion, this study reveals that natural mineral dust from the Gobi Desert, without any reprocessing, exhibits significant and stable catalytic properties regarding ozone decomposition for a large range of ozone concentrations (20 ppb–10 ppm) under atmospheric pressure. Determined catalytic decomposition rates exceed values observed on commonly used synthetic single metal oxides by one to two orders of magnitude, making natural mineral dust from the Gobi Desert a material of interest.

In addition to Gobi dust, natural dusts originating from other arid regions of the planet could also be efficient catalysts for ozone decomposition. Therefore, results experimentally evidence and bring to the foreground the concept of geocatalysis.

Funding: This research was funded by Chinese Scholarship Council grant number [201608070068], Labex, European Regional Development Fund (ERDF) and Région Hauts-de-France.

Acknowledgments: Authors acknowledge the China Scholarship Council (CSC) for the PhD grant attributed to Xianjie Wang, Labex Plas@Par and Ecole Polytechnique; IMT Lille Douai participates in the Labex CaPPA project funded by the ANR through the PIA under contract ANR-11-LABX-0005-01, and in the CLIMIBIO project, funded by the "Hauts-de-France" Regional Council and the European Regional Development Fund (ERDF).

Conflicts of Interest: The authors declare no conflict of interest. The funders had no role in the design of the study; in the collection, analyses, or interpretation of data; in the writing of the manuscript, or in the decision to publish the results.

References

1. Chameides, W.; Fehsenfeld, F.; Rodgers, M.; Cardelino, C.; Martinez, J.; Parrish, D.; Lonneman, W.; Lawson, D.; Rasmussen, R.; Zimmerman, P. Ozone precursor relationships in the ambient atmosphere. *J. Geophys. Res. Atmos.* **1992**, *97*, 6037–6055. [CrossRef]
2. Vingarzan, R. A review of surface ozone background levels and trends. *Atmos. Environ.* **2004**, *38*, 3431–3442. [CrossRef]
3. Bocci, V. Biological and clinical effects of ozone. Has ozone therapy a future in medicine? *Br. J. Biomed. Sci.* **1999**, *56*, 9–270.
4. Baysan, A.; Lynch, E. The use of ozone in dentistry and medicine. *Prim. Dent. Care* **2005**, *12*, 47–52. [CrossRef] [PubMed]
5. Thevenet, F.; Sivachandiran, L.; Guaitella, O.; Barakat, C.; Rousseau, A. Plasma-catalyst coupling for volatile organic compound removal and indoor air treatment: A review. *J. Phys. D Appl. Phys.* **2014**, *47*. [CrossRef]
6. Roland, U.; Holzer, F.; Kopinke, F.D. Combination of non-thermal plasma and heterogeneous catalysis for oxidation of volatile organic compounds: Part 2. Ozone decomposition and deactivation of γ-Al_2O_3. *Appl. Catal. B Environ.* **2005**, *58*, 217–226. [CrossRef]
7. Mehandjiev, D.; Naidenov, A. Ozone decomposition on α-Fe_2O_3 catalyst. *J. Int. Ozone Assoc.* **1992**, *14*, 277–282.
8. Klimovskii, A.; Bavin, A.; Tkalich, V.; Lisachenko, A. Interaction of ozone with γ-Al_2O_3 surface. *React. Kinet. Catal. Lett.* **1983**, *23*, 95–98. [CrossRef]
9. Bulanin, K.; Lavalley, J.; Tsyganenko, A. Ir spectra of adsorbed ozone. *Colloids Surf. A Physicochem. Eng. Asp.* **1995**, *101*, 153–158. [CrossRef]
10. Thomas, K.; Hoggan, P.; Mariey, L.; Lamotte, J.; Lavalley, J. Experimental and theoretical study of ozone adsorption on alumina. *Catal. Lett.* **1997**, *46*, 77–82. [CrossRef]
11. Sullivan, R.; Thornberry, T.; Abbatt, J. Ozone decomposition kinetics on alumina: Effects of ozone partial pressure, relative humidity and repeated oxidation cycles. *Atmos. Chem. Phys.* **2004**, *4*, 1301–1310. [CrossRef]
12. Dhandapani, B.; Oyama, S.T. Kinetics and mechanism of ozone decomposition on a manganese oxide catalyst. *Chem. Lett.* **1995**, *24*, 413–414. [CrossRef]
13. Jia, J.; Zhang, P.; Chen, L. Catalytic decomposition of gaseous ozone over manganese dioxides with different crystal structures. *Appl. Catal. B Environ.* **2016**, *189*, 210–218. [CrossRef]
14. Calderbank, P.; Lewis, J. Ozone-decomposition catalysis. *Chem. Eng. Sci.* **1976**, *31*, 1216. [CrossRef]
15. Alebić-Juretić, A.; Cvitaš, T.; Klasinc, L. Ozone destruction on powders. *Ber. Bunsenges. Phys. Chem.* **1992**, *96*, 493–495. [CrossRef]
16. Bulanin, K.; Alexeev, A.; Bystrov, D.; Lavalley, J.; Tsyganenko, A. IR study of ozone adsorption on SiO_2. *J. Phys. Chem.* **1994**, *98*, 5100–5103. [CrossRef]
17. Bulanin, K.; Lavalley, J.; Tsyganenko, A. Infrared study of ozone adsorption on CaO. *J. Phys. Chem. B* **1997**, *101*, 2917–2922. [CrossRef]
18. Bulanin, K.; Lavalley, J.; Tsyganenko, A. Infrared study of ozone adsorption on TiO_2 (anatase). *J. Phys. Chem.* **1995**, *99*, 10294–10298. [CrossRef]
19. Berlier, G.; Yamamoto, T.; Spoto, G.; Lamberti, C.; Gribov, E.; Zecchina, A. IR spectra of ozone adsorbed on MgO. *Phys. Chem. Chem. Phys.* **2002**, *4*, 3872–3875. [CrossRef]

20. Pangilinan, C.D.C.; Kurniawan, W.; Salim, C.; Hinode, H. Effect of Ag/TiO_2 catalyst preparation on gas-phase benzene decomposition using non-thermal plasma driven catalysis under oxygen plasma. *React. Kinet. Mech. Catal.* **2016**, *117*, 103–118. [CrossRef]
21. Perego, C.; Villa, P. Catalyst preparation methods. *Catal. Today* **1997**, *34*, 281–305. [CrossRef]
22. Winterton, N. *Chemistry for Sustainable Technologies: A Foundation*; Royal Society of Chemistry: London, UK, 2011.
23. Tang, M.; Cziczo, D.J.; Grassian, V.H. Interactions of water with mineral dust aerosol: Water adsorption, hygroscopicity, cloud condensation, and ice nucleation. *Chem. Rev.* **2016**, *116*, 4205–4259. [CrossRef] [PubMed]
24. Michel, A.; Usher, C.; Grassian, V. Reactive uptake of ozone on mineral oxides and mineral dusts. *Atmos. Environ.* **2003**, *37*, 3201–3211. [CrossRef]
25. Usher, C.; Michel, A.; Stec, D.; Grassian, V. Laboratory studies of ozone uptake on processed mineral dust. *Atmos. Environ.* **2003**, *37*, 5337–5347. [CrossRef]
26. Hanisch, F.; Crowley, J. Ozone decomposition on saharan dust: An experimental investigation. *Atmos. Chem. Phys.* **2003**, *3*, 119–130. [CrossRef]
27. Schoonen, M.A.; Xu, Y.; Strongin, D.R. An introduction to geocatalysis. *J. Geochem. Explor.* **1998**, *62*, 201–215. [CrossRef]
28. Romanias, M.N.; Ourrad, H.; Thevenet, F.; Riffault, V. Investigating the heterogeneous interaction of VOCs with natural atmospheric particles: Adsorption of limonene and toluene on saharan mineral dusts. *J. Phys. Chem. A* **2016**, *120*, 1197–1212. [CrossRef] [PubMed]
29. Goudie, A.; Middleton, N. Saharan dust storms: Nature and consequences. *Earth Sci. Rev.* **2001**, *56*, 179–204. [CrossRef]
30. Carlos-Cuellar, S.; Li, P.; Christensen, A.; Krueger, B.; Burrichter, C.; Grassian, V. Heterogeneous uptake kinetics of volatile organic compounds on oxide surfaces using a knudsen cell reactor: Adsorption of acetic acid, formaldehyde, and methanol on α-Fe_2O_3, α-Al_2O_3, and SiO_2. *J. Phys. Chem. A* **2003**, *107*, 4250–4261. [CrossRef]
31. Crowley, J.; Ammann, M.; Cox, R.; Hynes, R.; Jenkin, M.E.; Mellouki, A.; Rossi, M.; Troe, J.; Wallington, T. Evaluated kinetic and photochemical data for atmospheric chemistry: Volume v–heterogeneous reactions on solid substrates. *Atmos. Chem. Phys.* **2010**, *10*, 9059–9223. [CrossRef]
32. Kolb, C.; Cox, R.; Abbatt, J.; Ammann, M.; Davis, E.; Donaldson, D.; Garrett, B.C.; George, C.; Griffiths, P.; Hanson, D. An overview of current issues in the uptake of atmospheric trace gases by aerosols and clouds. *Atmos. Chem. Phys.* **2010**, *10*, 10561–10605. [CrossRef]
33. Tang, M.; Huang, X.; Lu, K.; Ge, M.; Li, Y.; Cheng, P.; Zhu, T.; Ding, A.; Zhang, Y.; Gligorovski, S. Heterogeneous reactions of mineral dust aerosol: Implications for tropospheric oxidation capacity. *Atmos. Chem. Phys.* **2017**, *17*, 11727–11777. [CrossRef]
34. Stephens, S.; Rossi, M.J.; Golden, D.M. The heterogeneous reaction of ozone on carbonaceous surfaces. *Int. J. Chem. Kinet.* **1986**, *18*, 1133–1149. [CrossRef]
35. Sheehy, D.P. A perspective on desertification of grazingland ecosystems in North China. *Ambio* **1992**, *21*, 303–307.
36. Romanias, M.N.; Zeineddine, M.N.; Gaudion, V.; Lun, X.; Thevenet, F.; Riffault, V. Heterogeneous interaction of isopropanol with natural gobi dust. *Environ. Sci. Technol.* **2016**, *50*, 11714–11722. [CrossRef] [PubMed]
37. Zeineddine, M.N.; Romanias, M.N.; Gaudion, V.; Riffault, V.; Thévenet, F. Heterogeneous interaction of isoprene with natural gobi dust. *ACS Earth Space Chem.* **2017**, *1*, 236–243. [CrossRef]
38. Romanias, M.N.; Zeineddine, M.N.; Riffault, V.; Thevenet, F. Isoprene heterogeneous uptake and reactivity on TiO_2: A kinetic and product study. *Int. J. Chem. Kinet.* **2017**, *49*, 773–788. [CrossRef]
39. Thevenet, F.; Olivier, L.; Batault, F.; Sivachandiran, L.; Locoge, N. Acetaldehyde adsorption on TiO_2: Influence of NO_2 preliminary adsorption. *Chem. Eng. J.* **2015**, *281*, 126–133. [CrossRef]
40. Batault, F.; Thevenet, F.; Hequet, V.; Rillard, C.; Le Coq, L.; Locoge, N. Acetaldehyde and acetic acid adsorption on TiO_2 under dry and humid conditions. *Chem. Eng. J.* **2015**, *264*, 197–210. [CrossRef]

© 2018 by the authors. Licensee MDPI, Basel, Switzerland. This article is an open access article distributed under the terms and conditions of the Creative Commons Attribution (CC BY) license (http://creativecommons.org/licenses/by/4.0/).